Effects of acidic calcium phosphate concentration on setting reaction and tissue response to β-tricalcium phosphate granular cement

Naoyuki Fukuda[1], Kunio Ishikawa[2], Kazuya Akita[1], Kumiko Kamada[1], Naito Kurio[1], Yoshihide Mori[3], Youji Miyamoto[1]

[1] Department of Oral Surgery, Oral Sciences, Clinical Dentistry, Institute of Biomedical Sciences, Tokushima University Graduate School, 3-18-15 Kuramoto-cho, Tokushima 770-8504, Japan

[2] Department of Biomaterials, Faculty of Dental Science, Kyushu University, 3-1-1 Maidashi, Higashi-ku, Fukuoka 812-8582, Japan

[3] Division of Maxillofacial Diagnostic and Surgical Sciences, Section of Oral and Maxillofacial Surgery, Faculty of Dental Science, Kyushu University, 3-1-1 Maidashi, Higashi, Fukuoka 812-8582, Japan

Corresponding author: Naoyuki Fukuda

Tel: +81-88-633-7354; Fax: +81-88-633-7462,

E-mail: naoyukifukuda@tokushima-u.ac.jp

Abstract

Beta-tricalcium phosphate granular cement (β-TCP GC), consisting of β-TCP granules and an acidic calcium phosphate (Ca-P) solution, shows promise in the reconstruction of bone defects as it sets to form interconnected porous structures, *i.e*., β-TCP granules are bridged with dicalcium phosphate dihydrate (DCPD) crystals. In this study, the effects of acidic Ca-P solution concentration (0–600 mmol/L) on the setting reaction and tissue response to β-TCP GC were investigated. The β-TCP GC set upon mixing with its liquid phase, based on the formation of DCPD crystals, which bridged β-TCP granules to one another. Diametral tensile strength of the set β-TCP GC was relatively the same, at approximately 0.6 MPa, when the Ca-P concentration was 20–600 mmol/L. Due to the setting ability, reconstruction of the rat's calvarial bone defect using β-TCP GC with 20, 200, and 600 mmol/L Ca-P solution was much easier compared to that with β-TCP granules without setting ability. Four weeks after the reconstruction, the amount of new bone was the same, approximately 17% in both β-TCP GC and β-TCP granules groups. Cellular response to β-TCP granules and β-TCP GC using the 20 mmol/L acidic Ca-P solution was almost the same. However, β-TCP GC using the 200 and 600 mmol/L acidic Ca-P solution showed a more severe inflammatory reaction. It is concluded, therefore, that β-TCP GC, using the 20 mmol/L acidic Ca-P solution, is recommended as this concentration allows surgical techniques to be performed easily and provides good mechanical strength, and the similar cellular response to β-TCP granules.

Keywords: Granular cement; β-tricalcium phosphate; Dicalcium phosphate dihydrate; Self-setting

INTRODUCTION

Reconstruction of bone defects using a calcium phosphate (Ca-P) bone augmentation material with interconnected porous structure is one of the key ways to obtain good clinical result as Ca-P exhibits osteoconductivity, and its porous structure allows cells and tissues to penetrate interior to the bone augmentation material [1-3]. At present, block type, granular type, and cement type bone augmentation materials are available. For the block type, while an interconnected porous structure is guaranteed, shaping the block to fit to the bone defect during the surgery is difficult, with improper shaping leading to lower bone to implant contact [4,5]. For the granular type, the defect is filled easily, and the granules form the interconnected porous structure. However, granules often migrate from the defect to the outside. In contrast, the cement type sets at the bone defect, and in this case, shaping is not necessary. Additionally, migration would not occur after setting. Therefore, porous cement has good potential to become an ideal bone augmentation material. Many attempts have been made to introduce pores in the cement. For example, Xu *et al*. (2001) introduced porogen into apatite forming cement [6-8]. However, dissolution of the porogen was not practical since it is time consuming.

We recently proposed an interconnected porous Ca-P cement. The cement consists of Ca-P granules and acidic solution. For example, β-tricalcium phosphate [β-TCP: β-$Ca_3(PO_4)_2$] granular cement (β-TCP GC) consists of β-TCP granules and monocalcium phosphate monohydrate [MCPM: $Ca(H_2PO_4)_2 \cdot H_2O$] saturated 0.6 mol/L of phosphoric acid solution. Upon mixing, dicalcium phosphate dihydrate [DCPD: $CaHPO_4 \cdot 2H_2O$] crystals are formed on the surface of β-TCP granules, and the DCPD crystals bridged the

β-TCP granules to one another, leading to the formation of an interconnected porous structure. Reconstruction surgery of the rat calvarial bone defect using the β-TCP GC was much easier compared to β-TCP granules. Four weeks after implantation, the amount of new bone formed at the β-TCP GC reconstructed bone defect area was comparable to those using pure β-TCP granules [9]. The β-TCP GC seems to have high potential value as a bone grafting material due to its self-setting ability, with the additional advantage of the osteoconductive behavior similar to that of β-TCP granules. The only potential problem could be the body's cellular response to implantation. In a previous study, MCPM saturated 0.6 mol/L of phosphoric acid solution was used as the liquid phase of β-TCP GC. Although new bone formation was not affected by the acidic solution, cellular response was more severe when compared to β-TCP granules.

Therefore, the objective of this study, was to evaluate the effects of Ca-P solution concentration on setting reaction and tissue response to the β-TCP GC.

MATERIALS AND METHODS

Preparation of β-TCP granules

β-TCP granules were prepared from calcium carbonate ($CaCO_3$, Wako Pure Chemical Industries Ltd., Osaka, Japan) and DCPD (Wako Pure Chemical) as reported previously [9,10]. In brief, $CaCO_3$ and DCPD powders were mixed homogeneously with 99.5% ethanol at a Ca/P ratio of 1.5 using a planetary ball mill (Pulverisette 5, Fritsch, Idar-Oberstein, Germany) at a speed of 200 rpm for 6 hours. The liquid was removed by filtration and air-dried. The dried powder was then placed in a stainless steel mold (φ30 mm) and pressed

uniaxially at 50 MPa using an oil-pressure press machine (MT-50HD, NPa System, Saitama, Japan). The obtained compacts were sintered at 1,100°C in a furnace (Super burn SBV1515D, Motoyama, Osaka, Japan) for 6 hours and then cooled inside the furnace. Sintered samples were then crushed and sieved so that the granule diameters would be between 300 and 600 μm.

Preparation of acidic Ca-P solution

The acidic Ca-P solutions were prepared by dissolving MCPM (Sigma-Aldrich Co., Saint Louis, USA) in phosphoric acid (H_3PO_4; Wako Pure Chemical) so that the solution would be saturated with respect to MCPM. The condition and pH of the acidic Ca-P solutions used in this study are summarized in Table 1. The concentration of H_3PO_4 used for the acidic Ca-P solution is used as the concentration of the acidic Ca-P solution for simple in the following text. The pH value of prepared acidic Ca-P solution was measured using a pH meter (D-51; Horiba Ltd., Kyoto, Japan) after calibration in accordance with the manufacturer's protocol.

β-TCP granular cement (β-TCP GC)

To prepare the β-TCP GC, β-TCP granules were mixed with the acidic Ca-P solution at a liquid-to-granule (L/G) ratio of 0.6. The mixture was packed in a splitting cylindrical mold (6 mm in diameter and 3 mm in height) with both ends of the mold covered by glass plates. After setting, the β-TCP GC was removed from the mold and immersed into acetone to stop the reaction. The concentration of the acidic Ca-P solution used for β-TCP GC is stated in parenthesis. For example, β-TCP GC (20) indicates β-TCP GC consisting of β-TCP granules and MCPM saturated 20 mmol/L H_3PO_4 solution.

Setting time measurement

Setting time of β-TCP GC was measured using a Vicat needle. After mixing the β-TCP granules with the acidic Ca-P solution, the mixture was placed into an inverted truncated cone mold. The mixture was pushed using a Vicat needle with 300 g weight, with the time until the Vicat needle could not penetrate the mixture measured at 10-second intervals.

Micro-computed tomography

The set β-TCP GC samples were scanned using micro-computed tomography (μ-CT) (Skyscan 1075 KHS; Skyscan, Kontich, Belgium) at a source voltage of 59 kV and source current of 169 μA using a 0.5 mm aluminum filter. The β-TCP GC was scanned using the middle-resolution scanning mode (18 μm voxel resolution) image.

Scanning electron microscopy

Morphology of the set β-TCP GC were observed using a scanning electron microscope (SEM: JCM-5700; JEOL Ltd., Tokyo, Japan) under an accelerating voltage of 15 kV after being coated with gold-palladium. Coating was performed using an ion coater (IB-3; Eiko engineering co., Ltd., Tokyo, Japan).

X-ray diffraction analysis

For compositional analysis, set β-TCP GC were ground into a fine powder and characterized using an X-ray diffractometer (XRD: D8 Advance; Bruker AXS GmbH, Karlsruhe, Germany) operated at 40 kV and 40 mA. The diffraction angle was continuously scanned in the 2θ range from 10° to 40° at a scanning rate of 2°/min. Quantitative analysis was performed based on the obtained XRD patterns. A calibration

curve for the quantitative analysis of DCPD was constructed using a mixture of DCPD ($2\theta = 11.78°$) and β-TCP ($2\theta = 31.18°$). The amount of DCPD in the set β-TCP GC was calculated from the integrated area ratio of the XRD peaks of DCPD to β-TCP using EVA15 software (Bruker AXS GmbH).

Mechanical strength measurement

The mechanical strength of the set β-TCP GC was evaluated in terms of diametral tensile strength (DTS). After drying the set β-TCP GC at room temperature, the diameter and height were measured with a micrometer (MDC-25MU: Mitutoyo Co. Ltd., Kanagawa, Japan). A load was then applied to crush the material using a universal testing machine (AGS-J 10kN; Shimadzu Co., Kyoto, Japan) at a constant cross-head speed of 1 mm/min. Mean and standard deviation (SD) for each DTS value was calculated using 8 samples.

Porosity measurement

Porosity was calculated from the bulk density of the set β-TCP GC and theoretical densities of β-TCP (3.07 g/cm^3) and DCPD (2.31 g/cm^3). The bulk density was measured from the external volume and weight of the set samples. The total porosity was calculated by following formulae (1) and (2).

$$\text{Relative density (\%)} = \text{Bulk density}/\text{Theoretical density} \times 100\ (\%) \quad (1)$$

$$\text{Total porosity (\%)} = 100 - \text{Relative density (\%)} \quad (2)$$

Surgical procedures

All animal experiments were conducted under approval of the Ethical Committee for Animal Experimentation at Tokushima University (Admission number: T29-81). Forty-eight male specific-pathogen-free (SPF) Wistar rats aged 12 weeks and weighing on average 350 to 400 g were used and randomly distributed into 4 groups of 12 rats: (1) β-TCP granules group, (2) β-TCP GC (20) group, (3) β-TCP GC (200) group, and (4) β-TCP GC (600) group. The β-TCP granules group employs just β-TCP granules, and were used as control. Each group was further divided into 2- and 4-week groups with 6 rats assigned to each group. The animals were administered general anesthesia with an intramuscular injection of 90 mg/kg ketamine hydrochloride and 10 mg/kg xylazine hydrochloride. After clipping the calvarial fur and disinfecting the surgical site using iodine, 2% (wt) lidocaine containing 1:80,000 epinephrine was injected subcutaneously for local anesthesia. Surgical incision through the skin and periosteum was performed at the calvaria, and then, a 9 mm artificial bone defect of calvarial bone was created by trephination under saline irrigation. After implantation of each sample, the periosteum and skin flap were repositioned and sutured using 4-0 nylon thread.

Histological evaluation

At 2- and 4 weeks post-implantation, the animals were euthanized and the calvarial bone was extracted and fixed with 10% (wt) formalin neutral buffer solution (Wako Pure Chemical). All samples were subjected to decalcification and routine histological processing, and then embedded in paraffin blocks. Samples were then sectioned horizontally at a thickness of 4 μm and stained with hematoxylin and eosin.

To evaluate the histological findings, all histological slides were observed using an

all-in-one microscope (BZ-X710, KEYENCE, Osaka, Japan). The percentage of newly formed bone and total cells in the defect was calculated from the area of newly formed bone and the area of total cells to the area of original defect created by trephination using image J software [11,12].

Statistical analysis

For statistical analysis, one-way factorial analysis of variance (ANOVA) and Fisher's least significant difference (LSD) post-hoc test were performed using Kaleida Graph 4. Values are expressed as means ± SD. $p < 0.05$ was considered statistically significant.

RESULTS

When β-TCP granules were mixed with the acidic Ca-P solutions, they set and formed an interconnected porous structure (Fig. 1 (b)-(d)). No significant difference was found regardless of the acidic Ca-P solution concentrations. The μ-CT analysis also confirmed the interconnected porous structure of the set β-TCP GC (Fig. 2 (a)-(c)). SEM observation revealed that the surface of the β-TCP granules were smooth, and typical for sintered Ca-P (Fig. 3 (a)). In contrast, the set β-TCP GC were covered with plate-like crystals, with the crystals interlocking, leading to the β-TCP granules to bridge one another (Fig. 3 (b)-(d)).

XRD analysis revealed that DCPD was formed in the set β-TCP GC (Fig. 4 (b)-(g)). Peak intensity ascribed to DCPD increased with concentration of the acidic Ca-P solution. The amount of DCPD formed in the set β-TCP GC was summarized as a function of acidic Ca-P concentration (Fig. 5). The amount of DCPD increased with the increase in

the concentration of acidic Ca-P, and was approximately 40% when the acidic Ca-P concentration was 20 mmol/L or higher. The setting time of β-TCP GC was approximately 1 min regardless of the acidic Ca-P solution concentration, even though setting time was slightly shorter when a higher concentration of acidic Ca-P solution was used (Table 2). Mechanical strength in terms of DTS of the set β-TCP GC increased with the acidic Ca-P concentration, reaching approximately 0.6 MPa when the acidic Ca-P concentration was 20 mmol/L or higher (Fig. 6). Porosity of the set β-TCP GC slightly decreased with increasing acidic Ca-P solution concentration up to 50 mmol/L. After which, the porosity became the same, at approximately 55%, up to at least 600 mmol/L (Fig. 7).

Fig. 8 shows typical histological images of the β-TCP granules, β-TCP GC (20), β-TCP GC (200), and β-TCP GC (600) 2 weeks post-implantation (a to d, respectively), as well as 4 weeks post-implantation (e to h, respectively). Amount of new bone and total cells are summarized in Fig. 9 and Fig. 10, respectively. At 2 weeks post-implantation, newly bony tissue was observed at both ends of the defect in both the β-TCP granules and the β-TCP GC. The amount of new bone formed was approximately 11%, with no significant difference observed between the β-TCP granules and the β-TCP GC, regardless of the acidic Ca-P solution concentration used for the liquid phase of β-TCP GC. Four weeks after implantation, bony tissue matured further in both β-TCP granules and β-TCP GC. The amount of new bone increased approximately 17%. Similarly, 4 weeks after implantation, no significant difference was observed between β-TCP granules and β-TCP GC.

In contrast to new bone formation, some histological differences were visually

observed between β-TCP granules and β-TCP GC. In β-TCP granules, slight lymphocytic infiltration was observed in the defect area 2 weeks after implantation, but this situation was observed to reduce 4 weeks after implantation. Similarly, β-TCP GC (20) showed slightly more lymphocyte infiltration 2 weeks after implantation, but with a reduction similar to β-TCP granules 4 weeks after implantation. On the other hand, β-TCP GC (200) and β-TCP GC (600) showed stronger lymphocytic infiltration when compared to β-TCP granules and β-TCP GC (20). In addition to the lymphocytic infiltration, granulation tissue and foreign body giant cells were clearly observed in both samples. Although foreign body giant cells were still observed 4 weeks after implantation, lymphocyte infiltration had decreased. Additionally, granulation tissue became fibrosis 4 weeks after implantation.

DISCUSSION

The results obtained in this study demonstrate that β-TCP granules set and form interconnected porous structure, even with a lower 20 mmol/L acidic Ca-P solution used as the liquid phase of β-TCP GC. The setting mechanism of the β-TCP GC has a close relationship with the DCPD crystals that precipitated on the surface of β-TCP granules. Upon mixing the β-TCP granules with an acidic Ca-P solution, β-TCP granules partially dissolve as shown in Equation (3). Dissolution of β-TCP results in an increase in Ca^{2+} and PO_4^{3-} concentration as well as in pH value, resulting in the solution becoming supersaturated with respect to DCPD. Therefore, DCPD crystals are precipitated on the surface of β-TCP granules as shown in Equation (4).

dissolution: $\beta\text{-}Ca_3(PO_4)_2 \rightarrow 3Ca^{2+} + 2PO_4^{3-}$ (3)

precipitation: $Ca^{2+} + H^+ + PO_4^{3-} + 2H_2O \rightarrow CaHPO_4 \bullet 2H_2O$ (4)

The precipitated DCPD crystals on the surface of β-TCP granules bridge β-TCP granules to one another [9,10]. Although the amount of DCPD increased with the concentration of acidic Ca-P solution up to 20 mmol/L, no further DCPD increase was observed even when higher concentrations of acidic Ca-P solution were used. Similarly, DTS value increased with the acidic Ca-P solution concentration up to 20 mmol/L, with no further DTS increase observed even when higher concentrations of acidic Ca-P solution were used. As shown in Fig. 3, all surfaces of the β-TCP granules were covered with the DCPD crystals when mixed with 20 mmol/L acidic Ca-P solution. This could be the reason as to why the amount of DCPD and DTS value were not influenced by the higher concentration of the acidic Ca-P solution. If so, unreacted acidic Ca-P solution will remain inside the set β-TCP GC when acidic Ca-P solution higher than 20 mmol/L is employed as the liquid phase of β-TCP GC.

Interestingly, the amount of new bone formed was same between β-TCP granules and β-TCP GC despite the concentration of acidic Ca-P solution, and as shown in Figure 9. In contrast to new bone formation, cellular response was different based on the concentration of the acidic Ca-P solution. The amount of total cells were the same between β-TCP granules and β-TCP GC (20) for 2 and 4 weeks after implantation. However, both β-TCP GC (200) and β-TCP GC (600) showed statistically ($p<0.05$) higher

total cell number than β-TCP granules. These results may indicate that redundant acid is simply the factor causing an increase in the inflammatory response [13-16]. Although new bone formation was not affected by the excess acidic Ca-P solution, excess acidic Ca-P solution should be avoided to prevent an unnecessary possible inflammatory response.

CONCLUSION

It was found that 20 mmol/L of acidic Ca-P solution was enough for the DCPD formation and bridging the β-TCP granules with the DCPD precipitation. Although the amount of new bone was similar among β-TCP granules, β-TCP GC (20), β-TCP GC (200), and β-TCP GC (600), β-TCP GC (20) should be used since cellular response to β-TCP GC (20) was similar to β-TCP granules, whereas β-TCP GC (200) and β-TCP GC (600) showed stronger lymphocyte infiltration.

ACKNOWLEDGEMENTS

This study was supported by AMED (Grant Number 18im0210810h0002), and Japan Society for the Promotion of Science (JSPS) KAKENHI (Grant Number JP17H06910).

REFERENCES

1. Loh QL, Choong C. Three-Dimensional Scaffolds for Tissue Engineering Applications: Role of Porosity and Pore Size. Tissue Eng Part B Rev 2013;19(6):485-502.
2. Hollister SJ. Porous scaffold design for tissue engineering. Nat Mater 2005;4(7):518-524.
3. Zhang YS, Zhu C, Xia Y. Inverse Opal Scaffolds and Their Biomedical Applications. Adv Mater 2017;29(33).
4. Theiss F, Apelt D, Brand B, Kutter A, Zlinszky K, Bohner M, Matter S, Frei C, Auer JA, von Rechenberg B. Biocompatibility and resorption of a brushite calcium phosphate cement. Biomaterials 2005;26:4383-4394.
5. Niedhart C, Maus U, Redmann E, Siebert CH. *In vivo* testing of a new *in situ* setting beta-tricalcium phosphate cement for osseous reconstruction. J Biomed Mater Res 2001;55(4):530-537.
6. Xu HH, Quinn JB, Takagi S, Chow LC, Eichmiller FC. Strong and macroporous calcium phosphate cement: Effects of porosity and fiber reinforcement on mechanical properties. J Biomed Mater Res 2001;57(3):457-466.
7. Xu HH, Takagi S, Quinn JB, Chow LC. Fast-setting calcium phosphate scaffolds with tailored macropore formation rates for bone regeneration. J Biomed Mater Res A 2004;68(4):725-734.
8. Zhang Y, Xu HH, Takagi S, Chow LC. In-situ hardening hydroxyapatite-based scaffold for bone repair. J Mater Sci Mater Med 2006;17(5):437-445.

9. Fukuda N, Tsuru K, Mori Y, Ishikawa K. Fabrication of self-setting β-tricalcium phosphate granular cement. J Biomed Mater Res Part B App Biomater 2018;106(2):800-807.
10. Fukuda N, Tsuru K, Mori Y, Ishikawa K. Effect of citric acid on setting reaction and tissue response to β-TCP granular cement. Biomed Mater 2017;12(1):015027.
11. Abramoff MD, Magelhaes PJ, Ram SJ. Image Processing with ImageJ. Biophotonics International 2004;11(7):36-42.
12. Schneider CA, Rasband WS, Eliceiri KW. NIH Image to ImageJ: 25 years of image analysis. Nature Methods 2012;9(7):671-675.
13. Yokoyama A, Yamamoto S, Kawasaki T, Kohgo T, Nakasu M. Development of calcium phosphate cement using chitosan and citric acid for bone substitute materials. Biomaterials 2002;23(4):1091-1101.
14. Kurashina K, Ogiso A, Kotani A, Takeuchi H, Hirano M. Histological and microradiographic evaluation of hydrated and hardened alpha-tricalcium phosphate/calcium phosphate dibasic mixtures. Biomaterials 1994;15(6):429-432.
15. Kurashina K, Kurita H, Kotani A, Kobayashi S, Kyoshima K, Hirano M. Experimental cranioplasty and skeletal augmentation using an alpha-tricalcium phosphate/dicalcium phosphate dibasic/tetracalcium phosphate monoxide cement: preliminary short-term experiment in rabbits. Biomaterials 1998;19(7-9):701-706.
16. Miyamoto Y, Ishikawa K, Takeuchi M, Toh T, Yoshida Y, Nagayama M, Kon M, Asaoka K. Tissue response to fast-setting calcium phosphate cement in bone. J Biomed Mater Res 1997;37(4):457-464.

Figure legends

Figure 1 Typical photographs of (a) β-TCP granules, (b) set β-TCP GC (20), (c) β-TCP GC (200), and (d) β-TCP GC (600).

Figure 2 Typical μ-CT images of (a) β-TCP granules, (b) set β-TCP GC (20), (c) β-TCP GC (200), and (d) β-TCP GC (600).

Figure 3 Typical SEM images of (a) β-TCP granules, (b) set β-TCP GC (20), (c) β-TCP GC (200), and (d) β-TCP GC (600).

Figure 4 XRD patterns of (a) β-TCP granules and (b) set β-TCP GC (0), (c) β-TCP GC (20), (d) β-TCP GC (200), and (e) β-TCP GC (600). XRD pattern of standard DCPD is shown as a reference (: ● DCPD,: ▼ β-TCP).

Figure 5 Amount of DCPD in the set β-TCPGC as a function of acidic Ca-P solution concentration. These values were calculated from the XRD patterns (n=4).

Figure 6 DTS value of the set β-TCP GC as a function of the acidic Ca-P solution concentration(n=8).

Figure 7 Porosity of the set β-TCP GC as a function of the acidic Ca-P solution concentration (n=8).

Figure 8 Histological images of (a) and (e) β-TCP granules; (b) and(f) β-TCP GC (20); (c) and (g) β-TCP GC (200); (d) and (h) β-TCP GC (600) at 2- and 4- weeks after implantation. (a)-(d) 2-weeks after implantation; (e)-(h) 4-weeks after implantation. Hematoxylin and eosin stain. Scale bar indicates 1000 μm.

Figure 9 Amount of new bone in the defect at 2- and 4-weeks after implantation (n=6).

Figure 10 Amount of total cells in the bone defect at 2- and 4-weeks after implantation ($^{*}p < 0.05$) (n = 6).

Table 1. Composition of respective acidic Ca-P solution and concentration of Ca^{2+}, PO^{4-} ions, and its pH in the respective solution.

Concentration (mmol/L)		Concentration (mmol/L)		pH
H_3PO_4	MCPM	Ca^{2+}	PO_4^{3-}	
0	200	200	400	1.99
10	220	220	450	1.58
20	230	230	480	1.59
30	240	240	520	1.58
50	270	270	590	1.58
100	330	330	770	1.58
150	400	400	950	1.50
200	460	460	1130	1.48
600	980	980	2570	1.42

Table 2. Setting time of β-TCP GC with respective concentration of acidic Ca-P solution.

Concentration of H_3PO_4 (mmol/L)	Setting time (min)
0	1.8 ± 0.3
10	1.8 ± 0.4
20	1.7 ± 0.1
30	1.4 ± 0.2
50	1.2 ± 0.2
100	1.3 ± 0.1
150	1.3 ± 0.1
200	1.2 ± 0.1
600	1.1 ± 0.2

Figure 1

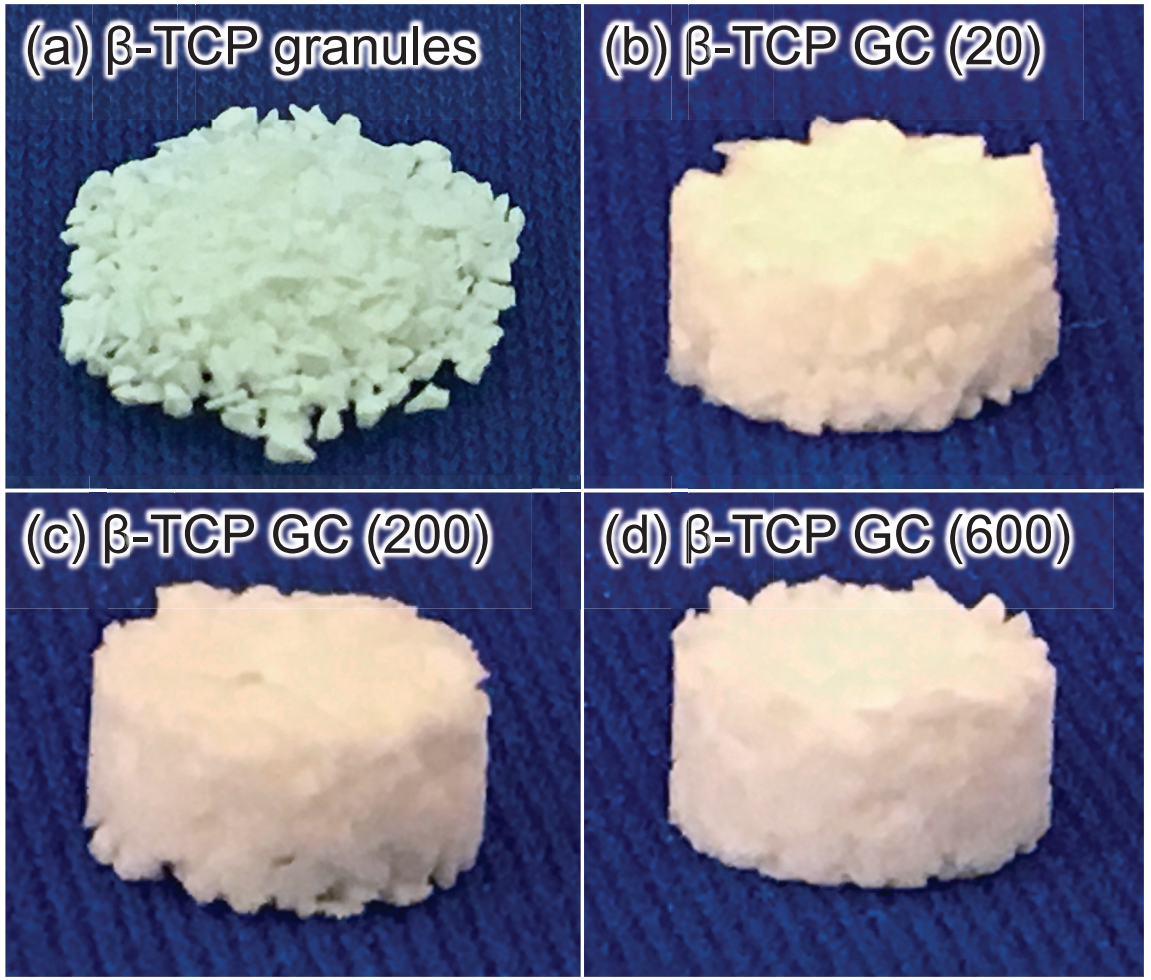

Fig. 1 Typical photographs of (a) β-TCP granules, (b) set β-TCP GC (20), (c) β-TCP GC (200), and (d) β-TCP GC (600).

Figure 2

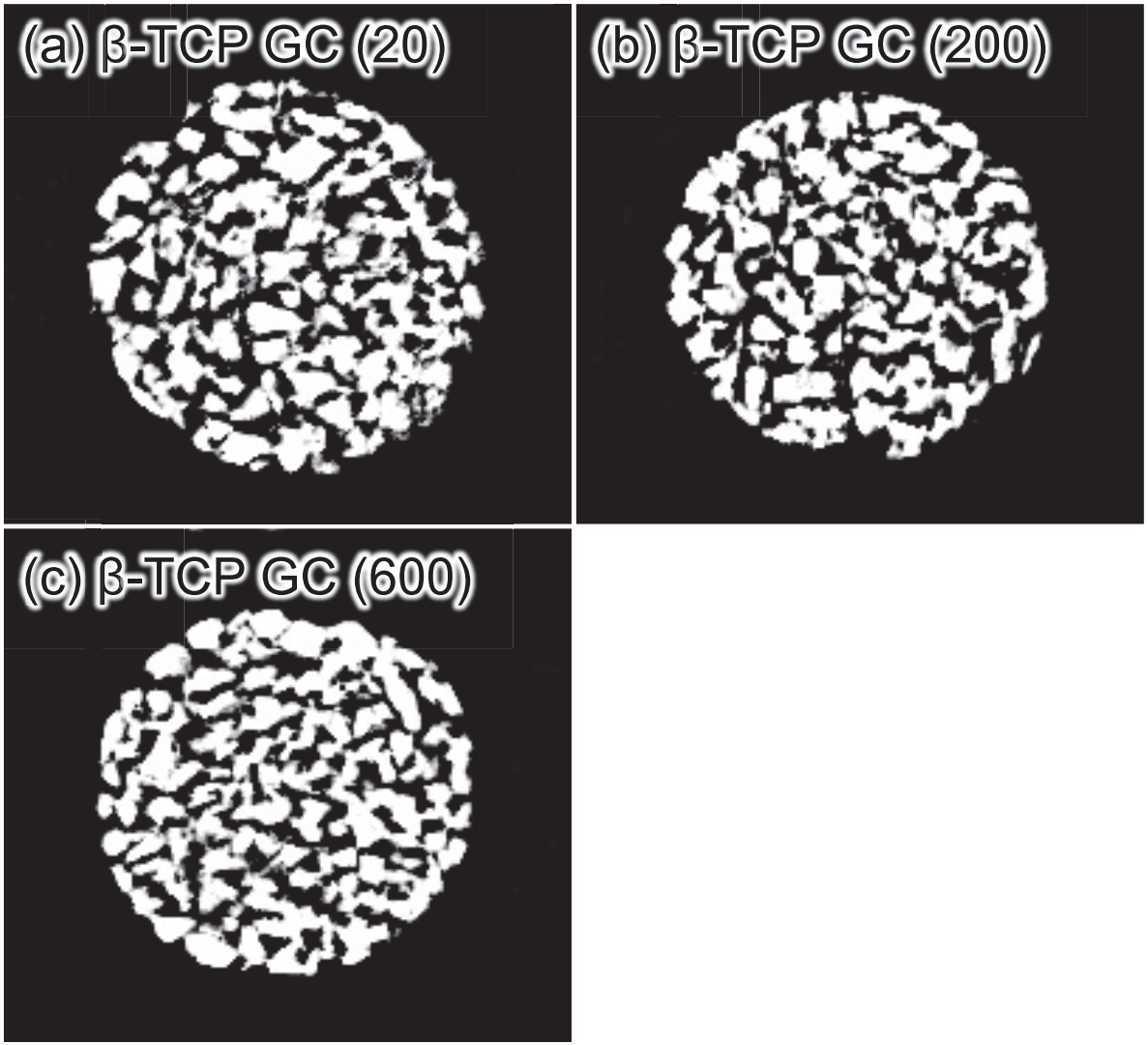

Fig. 2 Typical μ-CT images of (a) β-TCP granules, (b) set β-TCP GC (20), (c) β-TCP GC (200), and (d) β-TCP GC (600).

Figure 3

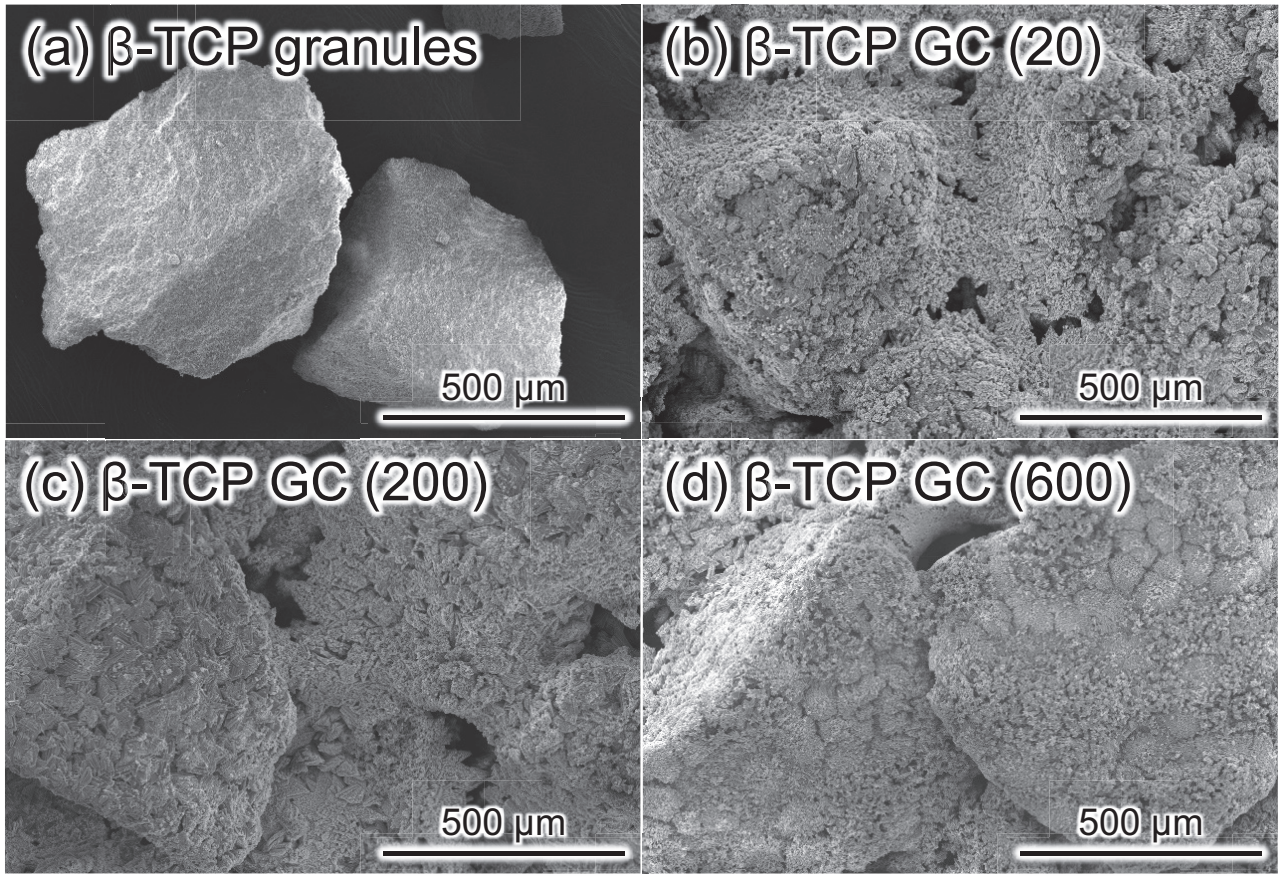

Fig. 3 Typical SEM images of (a) β-TCP granules, (b) set β-TCP GC (20), (c) β-TCP GC (200), and (d) β-TCP GC (600).

Figure 4

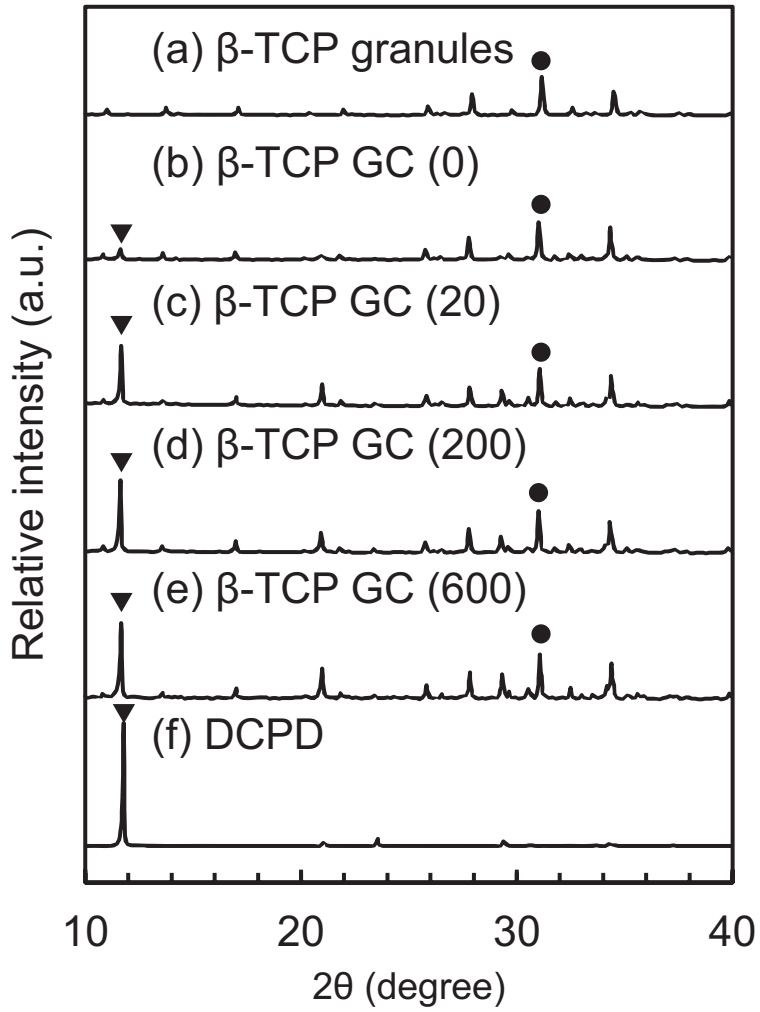

Fig. 4 XRD patterns of (a) β-TCP granules and (b) set β-TCP GC (0), (c) β-TCP GC (20), (d) β-TCP GC (200), and (e) β-TCP GC (600). XRD pattern of standard DCPD is shown as a reference (: ● DCPD,: ▼ β-TCP).

Figure 5

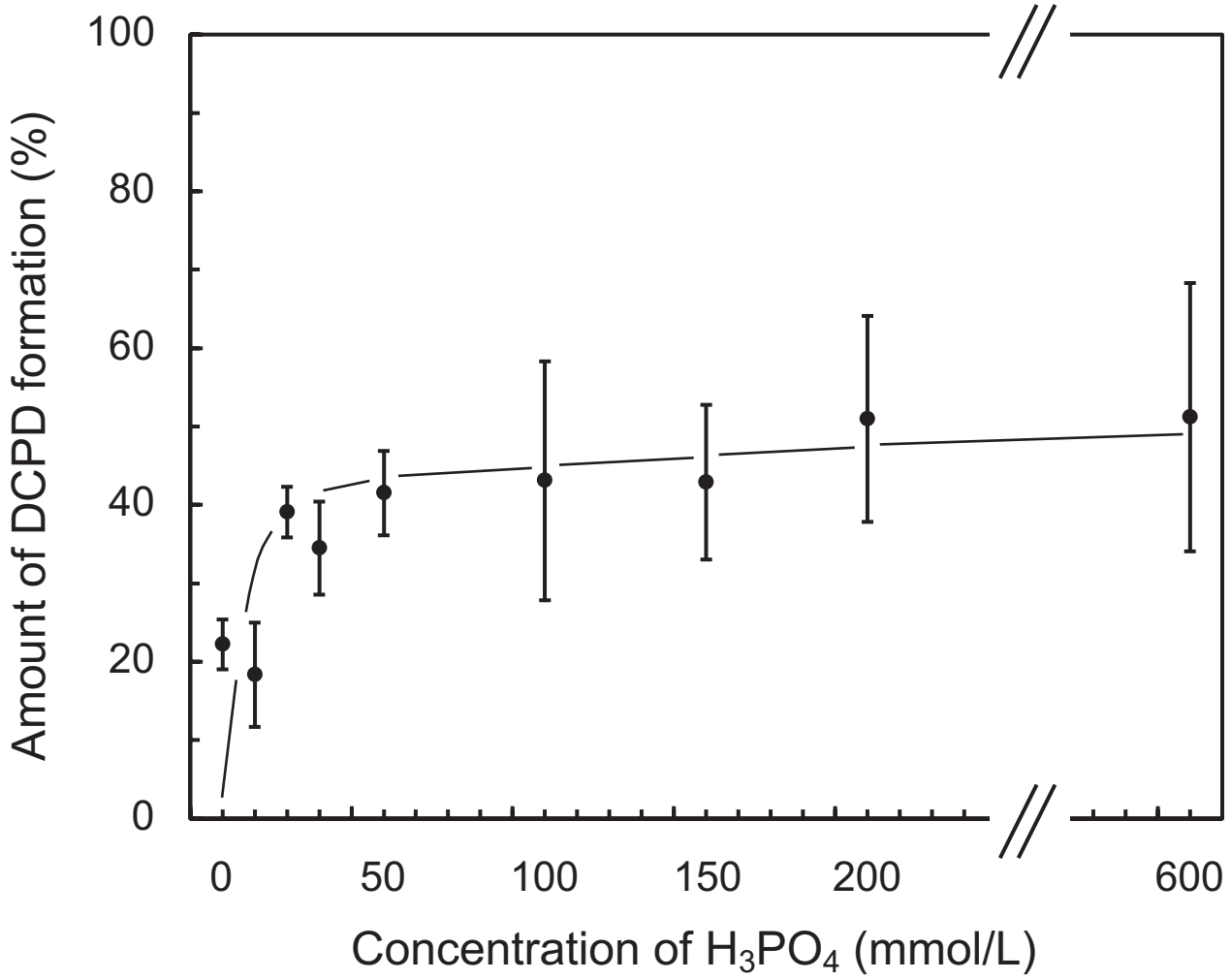

Fig. 5 Amount of DCPD in the set β-TCPGC as a function of acidic Ca-P solution concentration. These values were calculated from the XRD patterns. (n=4)

Figure 6

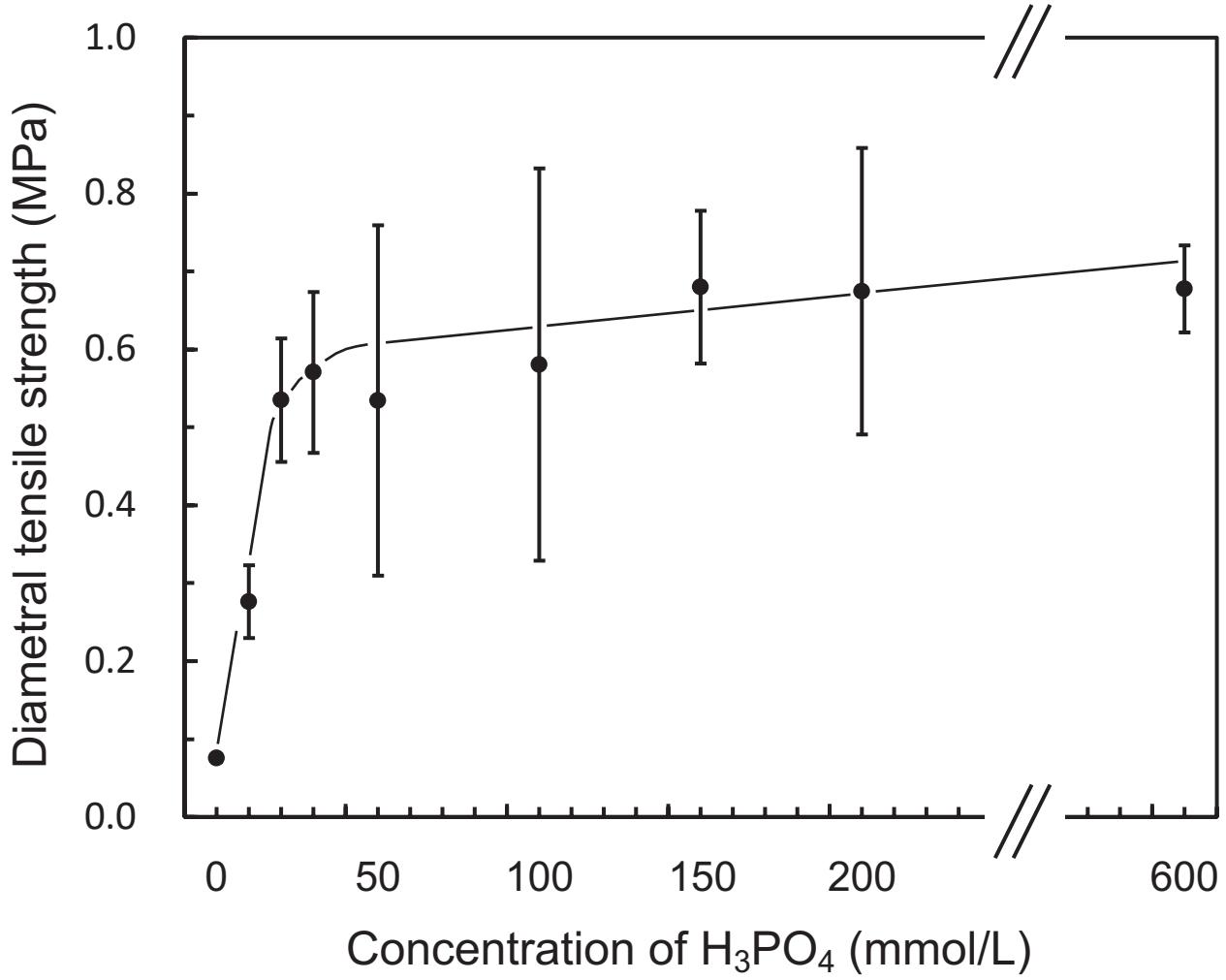

Fig.6 DTS value of the set β-TCP GC as a function of the acidic Ca-P solution concentration. (n=8)

Figure 7

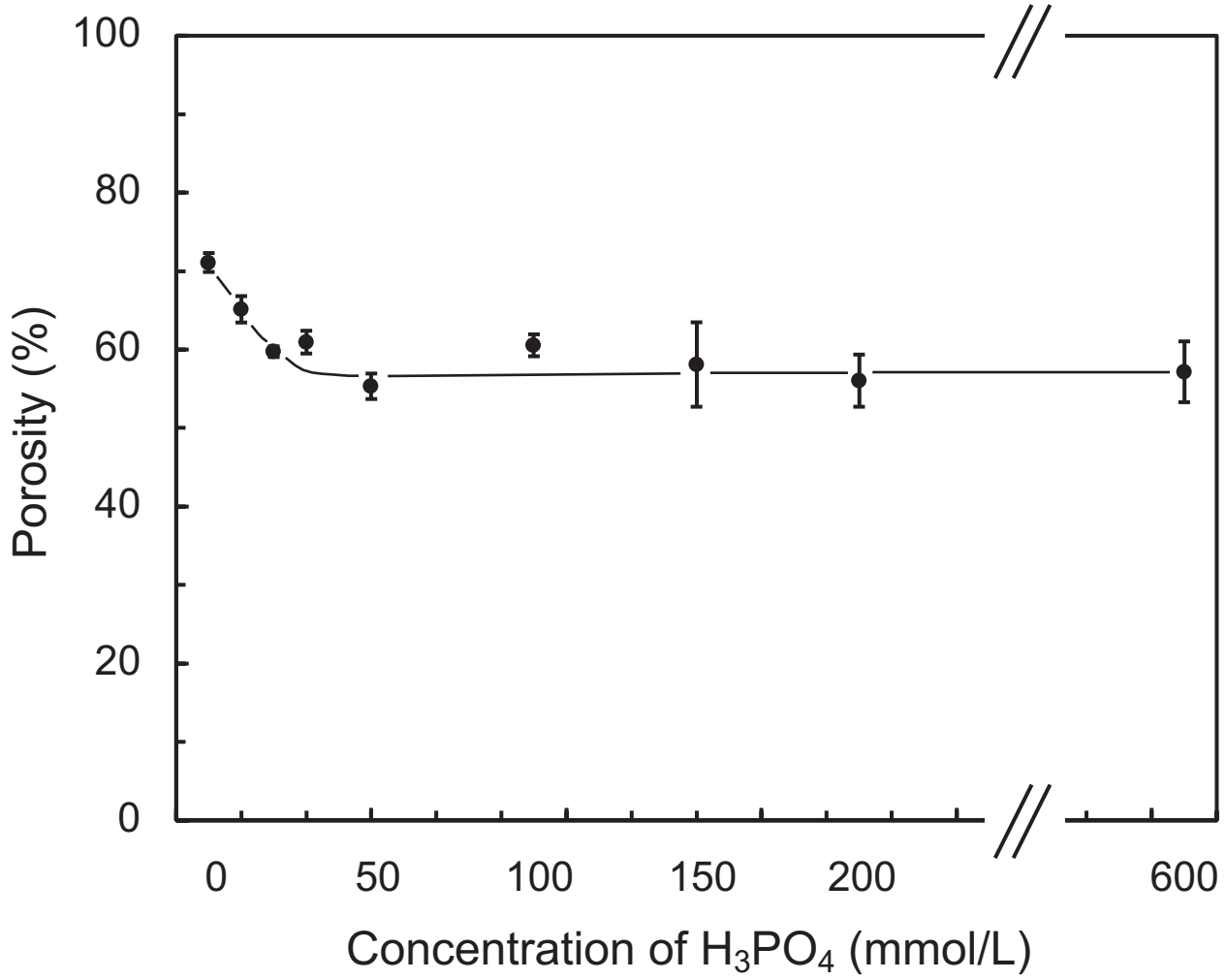

Fig. 7 Porosity of the set β-TCP GC as a function of the acidic Ca-P solution concentration. (n=8)

Figure 8

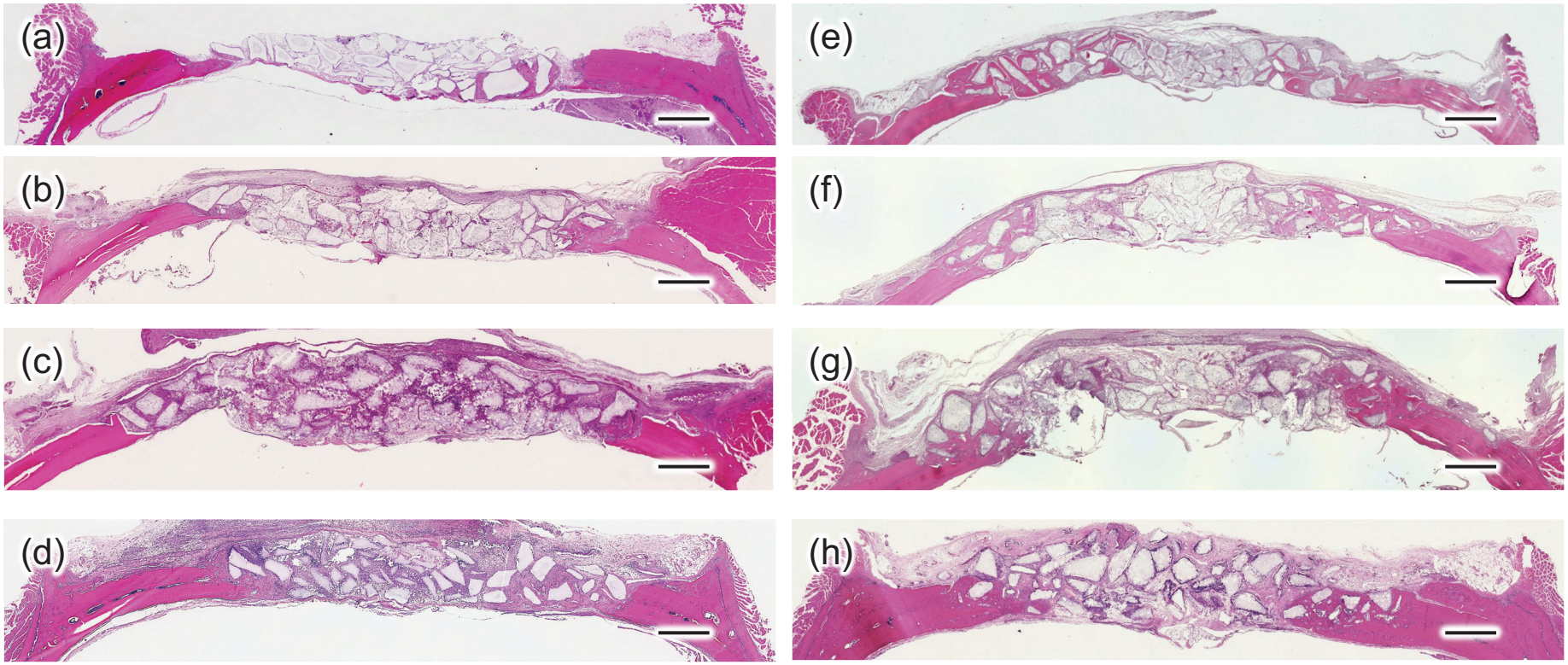

Fig. 8 Histological images of (a), (e) β-TCP granules, (b), (f) β-TCP GC (20), (c), (g) β-TCP GC (200), (d), (h) β-TCP GC (600) at 2 and 4 weeks after implantation. (a)-(d) 2 weeks after implantation; (e)-(h) 4 weeks after implantation. (hematoxylin and eosin stain). Scale bar indicates 1000 μm.

Figure 9

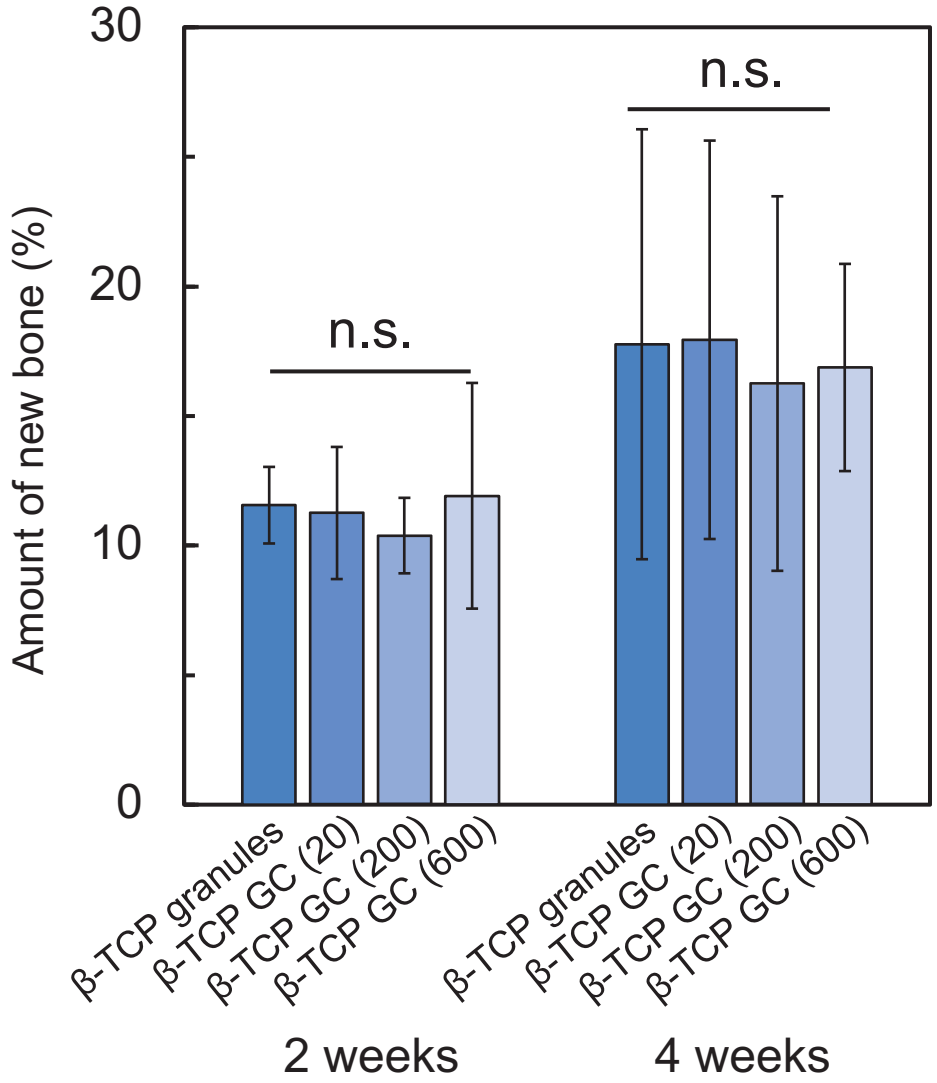

Fig. 9 Amount of new bone in the defect at 2 and 4 weeks after implantation. (n=6)

Figure 10

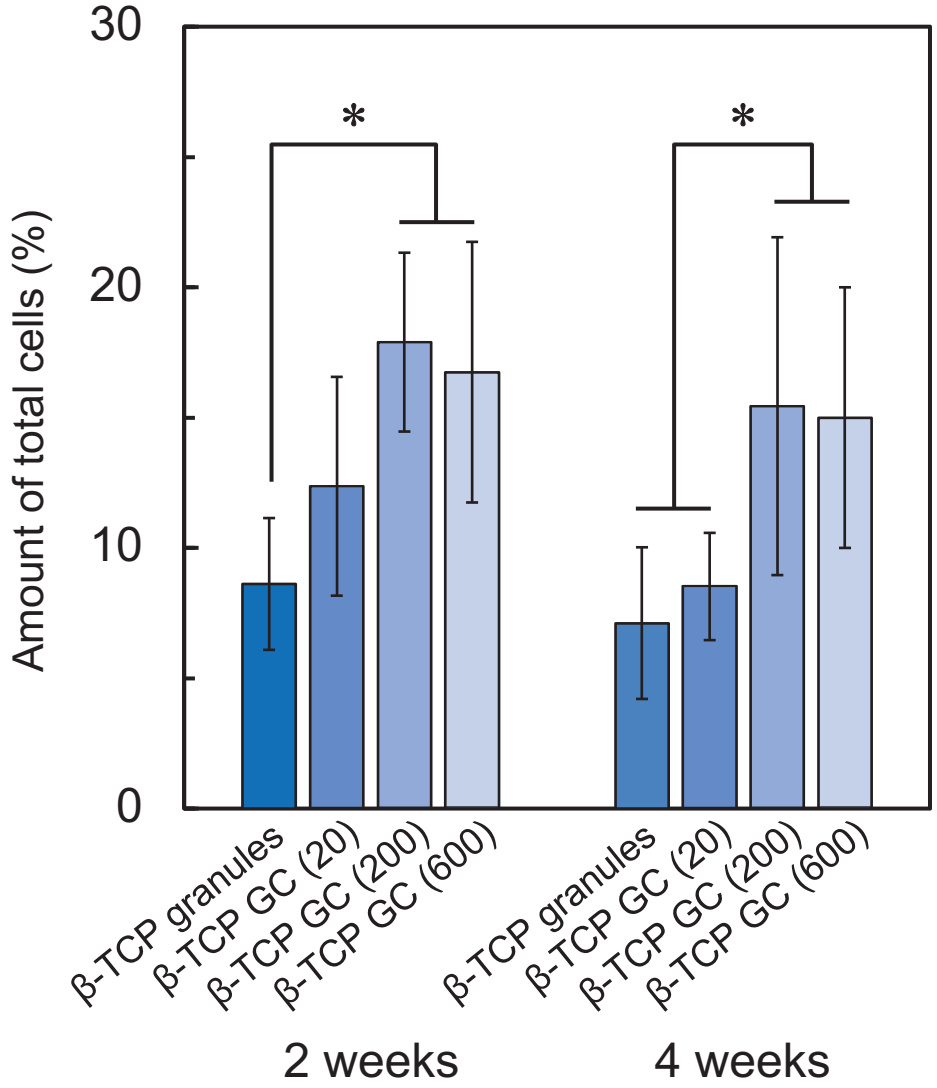

Fig. 10 Amount of total cells in the bone defect at 2 and 4 weeks after implantation (＊p＜ 0.05). (n = 6)